Psychotic-like experiences, polygenic risk scores for schizophrenia and structural properties of the salience, default mode and central-executive networks in healthy participants from UK Biobank

Alloza C.[1,2,3,4] Blesa-Cábez M.[5], Bastin M.E.[6,7] Madole J.W.[8], Buchanan C.R.[7,9], Janssen J.[2,3,4], Gibson J.[1], Deary I.J.[7], Tucker-Drob E.M.[8], Whalley H.C.[1], Arango C.[2,3,4,10], McIntosh A.M[1,7], Cox S.R[7,9]* and Lawrie S.M[1]*

[1] Department of Psychiatry, The University of Edinburgh, Edinburgh, United Kingdom

[2] Department of Child and Adolescent Psychiatry, Institute of Psychiatry and Mental Health, Hospital General Universitario Gregorio Marañón, Madrid, Spain

[3] Instituto de Investigación Sanitaria Gregorio Marañón (IiSGM), Madrid, Spain

[4] Ciber del Area de Salud Mental (CIBERSAM), School of Medicine, Madrid, Spain

[5] MRC Centre for Reproductive Health, The University of Edinburgh, Edinburgh, United Kingdom

[6] Centre for Clinical Brain Sciences, The University of Edinburgh, Edinburgh, United Kingdom

[7] Centre for Cognitive Ageing and Cognitive Epidemiology, Department of Psychology, The University of Edinburgh, Edinburgh, United Kingdom

[8] Department of Psychology, University of Texas at Austin, Austin, USA

[9] Scottish Imaging Network: A Platform for Scientific Excellence (SINAPSE)

[10] School of Medicine, Universidad Complutense, Madrid, Spain

Corresponding author: clara.alloza@gmail.com

* authors contributed equally

Abstract

Schizophrenia is a highly heritable disorder with considerable phenotypic heterogeneity. Hallmark psychotic symptoms can be considered as existing on a continuum from non-clinical to clinical populations. Assessing genetic risk and psychotic-like experiences (PLEs) in non-clinical populations and their associated neurobiological underpinnings can offer valuable insights into symptom-associated brain mechanisms without the potential confounds of the effects of schizophrenia and its treatment. We leveraged a large population-based cohort (UKBiobank) including information on PLEs, polygenic risk scores for schizophrenia (szPGRS) and multi-modal brain imaging in combination with network neuroscience. Morphometric (cortical thickness, volume) and water diffusion (fractional anisotropy) properties of the regions and pathways belonging to the salience, default-mode and central-executive networks were computed. We hypothesized that these anatomical concomitants of functional dysconnectivity would be negatively associated with szPGRS and PLEs. SzPGRS was associated with a latent measure of cortical thickness across the salience network ($r = -0.069$, $p = 0.010$) and with the right insular cortex ($\beta = -0.046$, $p_{FDR} = 0.050$). Moreover, PLEs showed a number of significant positive and negative associations with morphometric properties of the salience and default mode networks ($p_{FDR} < 0.050$); with the cortical thickness of the insula largely mediating the relationship between szPGRS and unusual voices. These results are consistent with the hypothesis that higher genetic liability for schizophrenia is related to subtle disruptions in brain structure and predisposes to PLEs even among healthy participants. In addition, our study suggests that networks engaged during auditory verbal hallucinations show structural associations with PLEs in the general population.

Introduction

Schizophrenia is associated with a range of alterations in brain structure and function (1–4), some of which are related to a family history or specific genetic risk factors. Consistent relationships between delusions, hallucinations and brain structure and function have, however, proved elusive – potentially because of power issues in relatively small clinical samples and confounds such as antipsychotic drug exposure and substance abuse. Psychotic-like experiences (PLEs) of lesser severity are present not only in patients but also in 5-8% of the general population (5), and to some extent predict transition to psychiatric disorders among those with higher PLEs (6); with cohort studies supporting a continuity between subclinical and clinically significant psychotic symptoms (7, 8). Overall, evidence validates the study of the pathophysiology of these clinical phenotypes in non-clinical populations (9), with large studies from the general population also offering increased power to detect such effects.

Aberrant functioning and organization of the salience network, default mode network (DMN) and central-executive network (CEN) are core features of several psychiatric and neurological disorders (10); with patients diagnosed with schizophrenia showing structural and functional impairments in all three networks (11). The salience network includes the insula and anterior cingulate cortex and limbic regions, and is involved in the identification of biological and behaviourally relevant stimuli and the subsequent coordination of neural resources to guide flexible behaviour (12, 13). Aberrant intrinsic functional connectivity of the salience network has been observed in schizophrenia (14, 15) and in individuals at clinical high risk for psychosis (16), and is posited to underlie persecutory delusions in particular (17). The DMN is a distributed system of fronto-temporal-parietal cortex that is activated during passive cognitive states and deactivates during several cognitive tasks (18). The DMN is overactive in schizophrenia with significant correlations between the activity of subregions of the DMN and positive symptoms in schizophrenia (19); though the evidence is somewhat inconsistent (19–21). The CEN is a frontoparietal system coactivating the dorsolateral prefrontal cortex and the posterior parietal cortex during several cognitive tasks (22). Increased functional connectivity between the DMN and CEN has been linked to hallucinations in patients with schizophrenia (14).

Schizophrenia is highly polygenic, with many common alleles of small effect, and increasing numbers of genome-wide significant loci have been identified as sample sizes increase (23–25). Summary statistics from large-scale GWAS allow the degree of genetic liability for a heritable trait to be estimated in healthy subjects outside the population in which the original GWAS was conducted (26, 27). Only a small number of studies have analysed the relationship between polygenic risk score for schizophrenia (szPGRS) and neuroimaging biomarkers in healthy samples (26–31) but some of these associations map on to regions likely to be involved in the generation of psychotic symptoms and PLEs.

In this study, we investigated how szPGRS relate to neuroanatomical properties of the salience network, DMN and CEN and thence to PLEs. We computed the trajectories of water diffusion MRI parameters (using fractional anisotropy; FA), cortical thickness and grey matter volume of the regions involved in these networks in a large sample of healthy participants from UK Biobank in whom any such associations would not be confounded by illness-associated factors. In doing so, we employed a novel approach based on ROI-ROI analysis (derived from connectome processing) which extends our previous *a priori* network selection methods (32, 33), allowing a much finer-grained network approach than using other techniques which quantify white matter connectivity without direct subject-specific linkage to cortical or subcortical regions.

Methods

Participants

UK Biobank (http://www.ukbiobank.ac.uk/) comprises around 500,000 community-dwelling participants recruited from across the United Kingdom of Great Britain and Northern Ireland between 2006 and 2014. A subset of the participants who were part of the initial recruitment attended for head MRI scanning at an average of around 4 years after the initial visit, on a MRI scanner in Manchester, UK (all data presented in this analysis were therefore collected on the same scanner). The current study uses the 5k neuroimaging data release (see Supplementary Material Figure 1). UK Biobank received ethical approval from the Research Ethics Committee (reference 11/NW/0382). Those participants who reported a diagnosis of schizophrenia or bipolar disorder with psychotic symptoms were excluded from our analysis. As an additional analysis, we excluded participants with any psychiatric diagnosis (diagnoses are presented in Supplementary Material Table 1). The present analyses were conducted as part of UK Biobank application 16124, linked to 4844 and 10279. All participants provided informed consent (http://biobank.ctsu.ox.ac.uk/crystal/field.cgi?id = 200).

Psychotic-like experiences information

Psychotic-like experiences (UKBiobank Category: 144) were categorised as conspiratorial thoughts, unusual signs or communications, unusual voices, and unusual visions (see Supplementary Material Methods 1). Participants that responded "do not know/prefer not to answer" were excluded from analyses in all cases.

Imaging analysis

Full details of the image acquisition and processing can be found on the UK Biobank website (http://biobank.ctsu.ox.ac.uk/crystal/refer.cgi?id=2367), Brain Imaging Documentation (http://biobank.ctsu.ox.ac.uk/crystal/refer.cgi?id=1977) and in (34). More information regarding scan acquisition, image processing and network construction can be found in Supplementary Material Methods 2 and Supplementary Material table 2 for a list of abbreviations of each node. Table 1 and

Figure 1 show the nodes and white matter pathways selected for each of the networks studied here. Details of polygenic risk score calculation are presented in Supplementary Material Methods 3. Our primary analyses used scores generated from a list of SNPs with a GWAS training set of $p \leq 0.1$ (results for 0.5 and 1.0 thresholds are presented in Supplementary Material Results 1). For the present study, data available for participants who were unrelated, survived the quality control process and had full imaging data available, is provided in Table 2.

[Table 1]

[Figure 1]

Statistical analyses

We undertook an *a priori* network-of-interest (NOI) approach, based on the literature cited above. Previous studies have suggested that schizophrenia is a syndrome of accelerated ageing (35), indicating for instance, significant declines in white matter coherence more than twice that of age-matched controls (36). Therefore, to examine accelerated brain ageing in brain structure, we included an interaction between age at MRI scanning and szPGRS in all analyses.

1. Linear regressions for individual network components

Initially, we conducted linear regressions between szPGRS and each node (thickness, volume) and edge (FA) within each of the selected NOIs. Within each model, each morphometric measure of each ROIs was set as the dependent variable, szPGRS at different thresholds as the independent variable, controlling for age, sex, and the interaction between age and szPGRS.

2. Network analyses

Next, we aimed to test whether associations with szPGRS were best represented in the data at the network-general level (common pathway), or whether there were additional unique associations with specific network components (common + independent pathways analysis), or whether the associations

were simply best described by independent pathways (37). We did so in a structural equation modelling (SEM) framework. First, we fitted measurement models (i.e. models that relate the latent factor to its manifest variables) to ascertain the degree to which we could describe overall network integrity at the network level; this initial measurement model was a confirmatory factor analysis in which we tried to estimate a single latent construct of global NOI "integrity" by incorporating altogether cortical and white matter metrics pertaining to all nodes within a NOI. However, these models all exhibited poor fit to the data, and the latent measures of the grey and white matter did not correlate significantly.

a) Common model analysis

Therefore, we opted to construct three measurement models for each NOI in which a latent factor was indicated by all network components separately: cortical grey matter thickness (derived from the bilateral cortical nodes), cortical grey matter volume (including all bilateral cortical and subcortical nodes), or white matter FA (derived from all pathways connecting bilateral nodes within each NOI). These measurement models all fitted the data well except for FA in the DMN and CEN networks which did not achieve acceptable model fit statistics and thus, were not included in these analyses.

For each model, we then tested associations between szPGRS and MRI parameters. We did so by fitting a multiple indicators, multiple causes (MIMIC) model (38); Figure 2 A shows a simplified diagram of the SEM framework. Within the model, each brain imaging measure was adjusted at the manifest level for its respective age, sex and either whole brain average cortical thickness, whole brain total grey matter volume (for volume) or whole brain mean FA, while szPGRS was adjusted for sex, population stratification components, genotyping array and the interaction between age and szPGRS. Model fits were assessed using the following indices and cut-offs: CFI, RMSEA and SRMR. We allowed for certain residual correlations between manifest variables in those cases in which their addition improved the model fit significantly. SEM analyses were conducted using the package 'lavaan' (39) in R with full-information maximum likelihood estimation to use all data available.

b) MIMIC common + independent pathways analysis

To assess whether associations between szPGRS and latent constructs of network integrity were best characterized at the global network level, or whether there were additional, specific, associations with particular brain regions beyond this, we ran a common plus independent pathways analysis (37) (see details of this analysis in supplementary Material Methods 4).

PLEs

Due to the high percentage of participants who did not answer to PLEs questionnaires (see Table 2), we first matched participants by age and sex with a ratio 1:10 using a propensity score method in the 'MatchIt' package (40). Linear regressions were then calculated using brain regions and each individual symptom as the response variable, covarying for either whole brain total grey matter volume (for node's volume; to control for differences in whole-brain volume across participants) or average cortical thickness (for node's cortical thickness; to control for differences in whole-brain cortical thickness across participants), age at MRI and sex. Raincloud plots (41) were used to plot group differences between participants with PLEs and their matched controls.

3. Mediation analyses

We further sought to formally test whether the association between szPGRS and PLEs was mediated by brain structure (at the manifest level). We did this in the form of a mediation model using the 'lavaan' package (39) with full-information maximum likelihood estimation, confidence intervals were reported (CI; constructed using 1000 bootstraps). This analysis was performed only in those cases where the path between brain structure (M) and PLEs (Y) was significant ($p_{FDR} < 0.050$); mediation was observed when the change from σ to σ' was statistically significant (confidence intervals did not include zero). Within the model, each brain region was adjusted for age, sex and either average cortical thickness (cortical thickness analysis) or whole brain total grey matter volume (volume analysis). Figure 2 B shows a simplified diagram of the mediation framework.

[Figure 2]

4. Additional analyses

In order to determine whether the signal could be driven by any complication associated with any psychiatric disorder beyond a diagnosis of psychosis (i.e.: distress, dysfunction, co-morbidities, medication, unhealthy lifestyles, etc.), we excluded all participants with any psychiatric diagnosis from the PLEs analysis (results of these analyses can be found in Supplementary Material Results 2). In addition to this, due to the possible clinical significance of level of distress in relation to PLEs, we first computed logistic regressions with PLEs as the response variable and level of distress, age and sex as predictor variables. For those significant associations, we tested whether level of distress caused by PLEs could be mediating the relationship between brain structure and PLEs (results can be found in Supplementary Material Results 3). We also tested the hypothesis that increased number of PLEs was associated with a higher level of distress (42) (results can be found in Supplementary Material Results 4).

Throughout, analyses were performed in R (https://www.r-project.org) and standardised betas were reported throughout. For each section of statistical analysis, significance (p) values ($\alpha = 0.050$) were corrected for multiple comparisons using false discovery rate (FDR) (43).

Results

Participant characteristics are presented in Table 2, and PLE prevalence are presented in Supplementary Material Table 3. Mean values for cortical thickness and grey matter volumes for each node (according to the Desikan atlas (44)) are shown in Supplementary Figure 2. All SEM models showed acceptable fit to the data (fit indices are shown in Supplementary Material Table 4).

[Table 2]

SzPGRS ANALYSES

Salience Network

Linear regressions for individual network components

There were no significant associations between cortical and subcortical volumes and szPGRS (p_{FDR} > 0.050). However, for cortical thickness, a significant negative association was found between the right insula and szPGRS (β = -0.046, SE = 0.019, p_{FDR} = 0.050). Left insula thickness and szPGRS was nominally significant and in the same direction but did not survive FDR-correction (β = -0.039, SE = 0.018, p_{FDR} = 0.065). Interactions between age and szPGRS were significant for cortical thickness of the right caudal anterior cingulate (CAC) (β = -0.054, SE = 0.021, p_{FDR} = 0.040). However, there were no significant associations between white matter FA and szPGRS (p_{FDR} > 0.050).

MIMIC common + independent pathways analysis

The associations between the latent factor for grey matter volume and szPGRS were not significant (r = -0.026, SE = 0.014, p = 0.242). Allowing for a direct effect of szPGRS on left thalamus volume significantly improved model fit ($\chi^2[1] > 4.917$, $p < 0.028$; independent pathway estimates: β = 0.017, p = 0.032). A direct effect of right CAC volume on szPGRS*age (β = -0.035, p = 0.088) –the second

independent pathway added – significantly improved model fit ($\chi^2[1] = 5.893$, $p = 0.015$) . Results are shown in Figure 3A.

In addition to the association between szPGRS and the latent factor of cortical thickness (r = -0.069, SE = 0.015, $p = 0.010$), an independent pathway emerged from szPGRS*age to right CAC thickness ($\beta = -0.043$, $p = 0.031$), which improved the model fit ($\chi^2[1] = 4.606$, $p = 0.03$; Figure 3B). There was no significant association between the latent factor for FA and either szPGRS or szPGRS*age interaction ($p > 0.050$).

[Figure 3]

Default Mode Network

Linear regressions for individual network components

There were no significant associations between grey matter volume, cortical thickness or white matter FA and szPGRS or the interaction between szPGRS*age ($p_{FDR} > 0.050$).

MIMIC common + independent pathways analysis

The associations between the latent factors for grey matter volume or thickness and szPGRS were not significant ($r_{volume} = -0.040$, SE = 0.012, $p = 0.111$; $r_{thickness} = -0.028$, SE = 0.015, $p = 0.273$). An independent pathway emerged from szPGRS*age to right supramarginal thickness ($\chi^2[1] > 5.705$, $p < 0.018$; independent pathway estimate: $\beta = -0.035$, $p = 0.008$). Interactions between szPGRS*age were not significantly associated with the latent constructs in the DMN ($p > 0.050$).

Central Executive Network

Linear regressions for individual network components

No significant associations were found between the volume, cortical thickness or FA and szPGRS at a threshold of $p \leq 0.1$, or the interaction between szPGRS*age ($p > 0.050$).

MIMIC common + independent pathways analysis

The associations between the latent factors for grey matter and szPGRS were not significant ($p > 0.050$). For the volumetric model, allowing for a direct effect of szPGRS on right inferior parietal volume ($\beta = 0.039$, $p = 0.004$) resulted in significant improvement in model fit ($\chi^2[1] > 7.741$, $p < 0.006$). For cortical thickness, an independent pathway emerged from szPGRS*age to right superior frontal thickness ($\chi^2[1] > 7.512$, $p < 0.007$; independent pathway estimate: $\beta = 0.028$, $p = 0.002$) and right inferior parietal thickness ($\chi^2[1] > 4.314$, $p < 0.039$; independent pathway estimate: $\beta = -0.024$, $p = 0.034$). Interactions between szPGRS*age were not significantly associated with any latent construct in the CEN ($p_{FDR} > 0.050$).

PSYCHOTIC SYMPTOMS

Table 2 shows the frequencies and percentages of respondents with PLEs, Supplementary Material Table 3 shows sample characteristics for participants reporting PLEs versus non-PLEs participants and a summary of results of associations between PLEs and structural properties is presented in Supplementary Material Table 5. Figure 4A shows raincloud plots representing differences in cortical thickness and volume between participants reporting PLEs and matched controls.

Salience Network

Significant negative associations were found between the thickness of the right and left insula and un-real voices ($N_{cases} = 51$, $N_{controls} = 510$; $\beta = -0.114$, SE = 0.035, $p_{FDR} = 0.004$ and $\beta = -0.083$, SE = 0.036, $p_{FDR} = 0.045$, respectively). Associations between total number of symptoms and cortical thickness/volume of salience network nodes were all non-significant.

Default Mode Network

A significant negative association was found between the volume of the right supramarginal gyrus and unusual signs (N_{cases} = 11, $N_{controls}$ = 110; β = -0.195, SE = 0.061, p_{FDR} = 0.022) and between conspiratorial thoughts and volume of the left pars orbitalis (N_{cases} = 12, $N_{controls}$ = 120; β = 0.219, SE = 0.069, p_{FDR} = 0.021). For conspiratorial thoughts, there was a positive association with the cortical thickness of the right supramarginal gyrus (N_{cases} = 13, $N_{controls}$ = 130; β = 0.177, SE = 0.048, p_{FDR} = 0.003). We did not find any significant association between total number of symptoms and volume/cortical thickness of nodes.

[Figure 4]

Central Executive Network

No significant associations were found for the other brain metrics of the CEN and PLEs (p_{FDR} > 0.050).

Mediation analyses

The mediation models using szPGRS and mediators met the criteria for close model fit (RMSEA = 0, CFI = 1, SRMR < 0.05). Standardised parameter estimates for the model are presented in Figure 5. We examined the hypothesis that higher szPGRS was associated with symptom severity via the brain structures significantly associated with PLEs in the salience and DMN. First, we tested the association between szPGRS and total number of symptoms in the whole UKBiobank sample, independently of diagnosis (N = 308,693). However, we did not find any significant association (β = 0.020, SE = 0.018, p = 0.283). We found that the linear association between szPGRS and unusual voices was significantly mediated by cortical thickness of the right insula (from σ = 0.023 to σ' = 0.004, CI [0.020, 0.127] with the right insular cortex mediating 82.61% of the association between szPGRS and voices). These results were consistent across all szPGRS thresholds (see Supplementary Material Results 5). No significant mediations were observed for any other ROIs.

[Figure 5]

Discussion

The present study aimed to investigate different structural properties of the salience, DMN and CEN networks in relation to szPGRS and PLEs in a large population-based cohort of healthy participants. This is, to our knowledge, the first study to investigate these polygenic-MRI associations using the structural properties of brain networks from a connectome perspective, where the properties of estimated connections that directly link distal cortical and subcortical regions in each individual are examined.

At the individual node level, we found that thinner right insular cortex was significantly associated with higher szPGRS. At the network level we found that greater genetic risk for schizophrenia was associated with reduced cortical thickness across the salience network, with some specific associations between genetic risk and individual brain properties emerging. The findings reported here indicate both global network and domain-specific pathways implicated in schizophrenia, indicating that those individual regions showing an independent significant association with szPGRS may be more susceptible/resilient to the effect of genetic risk beyond a latent factor of network integrity. Moreover, we found several significant associations between PLEs – in particular regarding auditory verbal hallucinations – and structural properties of the salience and DMN; with the right insular cortex largely mediating the association between voices and szPGRS.

Impairments in white matter micro- and macrostructure are a common feature in schizophrenia with healthy relatives who are genetically at higher risk of developing schizophrenia also exhibiting impairments in FA (45). These results are in accordance to a previous study, reporting non-significant associations between a general factor of FA (including 27 major white matter tracts across the brain) and szPGRS in a previous release of this UK Biobank data (n = 816) (46), though the current approach offers greater brain regional fidelity and statistical power. Despite the apparent impairments in white matter structure in schizophrenia, only a small number of studies have reported significant associations between genetic risk factors and white matter in healthy and clinical samples (28, 31, 47). Interestingly, significant reductions in global white matter volume in dizygotic twins discordant for schizophrenia have been reported while reductions in global grey matter were exclusively observed in patients diagnosed with schizophrenia (48). Thus, the null findings of white matter observed here may partly be

due to the aggregation of genetic and environmental risk factors found in affected individuals and their relatives compared with healthy individuals.

Psychotic-like experiences

Prevalences reported in this study were comparable to previous population studies (49, 50); with visual hallucinations being the most common PLEs followed by auditory hallucinations. The insula, with its important role in processing emotional and sensory stimuli is involved in interoception; this awareness of the body's internal state comprises emotional responses, complex cognitive states, and the sense of self (51, 52). An example of this is represented by patients with hallucinations making more errors in external attributions than those without hallucinations (53, 54). Consistent with our results, significant correlations between psychotic symptoms, activation, volume and surface area of the insula have been reported in clinical (55, 56) and high-risk samples (16); with hallucinations being the most correlated dimension with structural aspects of the insula (57). Our mediation analyses extend these findings by showing the cortical thickness of the right insula largely mediating the association between szPGRS and voices. This is in accordance with previous evidence suggesting that predominant right lateralization may discriminate auditory-verbal hallucinations from normal inner speech (58).

The supramarginal gyrus plays a key role in the auditory/phonological loop, a circuitry involved in processing auditory inputs, especially language (59); with lower volumes being related to auditory hallucinations in schizophrenia (60), while in non-psychotic individuals, auditory hallucinations have been linked to abnormal brain connectivity within the DMN and with auditory cortices (61, 62). The positive correlation between the volume of the right pars orbitalis, the ventral subregion of the inferior frontal gyrus, and conspiratorial thoughts is, however, at odds with previous studies reporting reduced volume of the pars orbitalis in high risk individuals (6, 63) and negative associations between the volume of this region and positive symptoms in clinical samples (64); suggesting that involvement of the pars orbitalis but not the inferior frontal gyrus – involved in language processing – may be limited to clinically-relevant populations.

Overall, extensive structural and functional neuroimaging literature supports our findings of the involvement of right supramarginal, bilateral insula and inferior frontal gyrus – all of them language-

related areas – in PLEs and of 'voices' in particular. Evidence indicates that those with auditory hallucinations tend to show impaired speech perception (65); with an engagement of both speech production and reception circuitry in participants experiencing auditory hallucinations in the scanner (66). As it has been suggested, voices tend to be the dominant content of auditory hallucinations because the human auditory system is tuned to the natural priors of speech (67); thus, in the context of this study, voices may be experienced as external communications, signs or conspiratorial thoughts since we regard voices to be accompanied by an agent.

Limitations

We limited our analysis to those networks implicated in previous functional and structural studies, translating those nodes onto a common parcellation scheme. Given issues of validity and comparability across brain atlases, and the implications of this for underlying connectivity (68–70), further research should aim to replicate this study by computing the networks at different levels of node granularity and with different structural properties. We applied a consistency-based thresholding method in an attempt to remove spurious white matter connections, exclusively preserving the top 30% that were most consistent across subjects. Though current evidence indicates that the human brain is likely to exhibit a fairly high degree of sparsity, principles of white matter connectivity in humans are not sufficiently comprehensive (when compared to the mouse, for example; (71)) to allow the confident implementation of detailed anatomical priors (72); some connections may have therefore been pruned erroneously. Finally, we investigated whether neurostructural properties of brain networks are associated with PLEs. Due to the relatively low frequencies of PLE in this sample, we decided to match participants. A previous study has indicated a potential "healthy volunteer" selection bias in this sample, suggesting that this cohort may not be representative of the sampling population (73).

Conclusions

In a large sample of largely healthy participants from UK Biobank a higher genetic liability for schizophrenia was associated with subtle neurostructural differences; in particular, a thinner cortex across the salience network, and in the insular cortex. Beyond these global relationships, some independent paths emerged in each structural network. We also found significant associations between PLEs and the insula, CAC, amygdala, supramarginal and inferior frontal gyrus; with the insula largely mediating the association between szPGRS and auditory hallucinations. Our results in a large healthy sample support previous studies on aberrant activation of language-related areas and the externalization of inner speech phenomena in clinical samples. The results of this research indicate that the study of the non-clinical phenotype represents a valid approach to investigate the pathophysiology of the clinical phenotype and suggest a shared genetic aetiology between the clinical and non-clinical phenotype.

Acknowledgements

We thank the UK Biobank participants for their participation and the UK Biobank team for their work in collecting, processing and disseminating these data for analysis. This research was conducted, using the UK Biobank Resource under approved project 16124 linked to 4844, in the Department of Psychiatry and Centre for Cognitive Ageing and Cognitive Epidemiology (CCACE) (http://www.ccace.ed.ac.uk) at The University of Edinburgh. SRC, SJR, JWM, MEB, CRB, IJD and EMT-D were supported by a National Institutes of Health (NIH) research grant R01AG054628. EMT-D was also supported by National Institutes of Health (NIH) research grant R01HD083613, and is a member of the Population Research Center at the University of Texas at Austin, which is supported by NIH center grant P2CHD042849. Also supported by the Spanish Ministry of Science, Innovation and Universities. Instituto de Salud Carlos III, co-financed by ERDF Funds from the European Commission, "A way of making Europe", CIBERSAM. Madrid Regional Government (B2017/BMD-3740 AGES-CM-2), European Union Structural Funds and European Union Seventh Framework Program and H2020 Program; Fundación Familia Alonso, Fundación Alicia Koplowitz and Fundación Mutua Madrileña.

Conflicts

Dr. Arango has been a consultant to or has received honoraria or grants from Acadia, Angelini, Gedeon Richter, Janssen Cilag, Lundbeck, Otsuka, Roche, Sage, Servier, Shire, Schering Plough, Sumitomo Dainippon Pharma, Sunovion and Takeda. In the last 3 years, Stephen M. Lawrie has received research support from Janssen and Lundbeck, and personal fees from Janssen and Sunovion

References

1. Kelly S, Jahanshad N, Zalesky A, Kochunov P, Agartz I, Alloza C, *et al.* (2017): Widespread white matter microstructural differences in schizophrenia across 4322 individuals: results from the ENIGMA Schizophrenia DTI Working Group. *Mol Psychiatry*. . doi: 10.1038/mp.2017.170.
2. Lawrie SM, Abukmeil SS (1998): Brain abnormality in schizophrenia. A systematic and quantitative review of volumetric magnetic resonance imaging studies. *Br J Psychiatry J Ment Sci*. 172: 110–120.
3. van Erp TGM, Walton E, Hibar DP, Schmaal L, Jiang W, Glahn DC, *et al.* (2018): Cortical Brain Abnormalities in 4474 Individuals With Schizophrenia and 5098 Control Subjects via the Enhancing Neuro Imaging Genetics Through Meta Analysis (ENIGMA) Consortium. *Biol Psychiatry*. . doi: 10.1016/j.biopsych.2018.04.023.
4. Wright IC, Rabe-Hesketh S, Woodruff PW, David AS, Murray RM, Bullmore ET (2000): Meta-analysis of regional brain volumes in schizophrenia. *Am J Psychiatry*. 157: 16–25.
5. van Os J, Linscott RJ, Myin-Germeys I, Delespaul P, Krabbendam L (2009): A systematic review and meta-analysis of the psychosis continuum: evidence for a psychosis proneness-persistence-impairment model of psychotic disorder. *Psychol Med*. 39: 179–195.
6. DeRosse P, Nitzburg GC, Ikuta T, Peters BD, Malhotra AK, Szeszko PR (2015): Evidence from structural and diffusion tensor imaging for frontotemporal deficits in psychometric schizotypy. *Schizophr Bull*. 41: 104–114.
7. Cannon M, Caspi A, Moffitt TE, Harrington H, Taylor A, Murray RM, Poulton R (2002): Evidence for early-childhood, pan-developmental impairment specific to schizophreniform disorder: results from a longitudinal birth cohort. *Arch Gen Psychiatry*. 59: 449–456.
8. Hanssen M, Bak M, Bijl R, Vollebergh W, van Os J (2005): The incidence and outcome of subclinical psychotic experiences in the general population. *Br J Clin Psychol*. 44: 181–191.
9. Kelleher I, Cannon M (2011): Psychotic-like experiences in the general population: characterizing a high-risk group for psychosis. *Psychol Med*. 41: 1–6.
10. Menon V (2011): Large-scale brain networks and psychopathology: a unifying triple network model. *Trends Cogn Sci*. 15: 483–506.
11. Palaniyappan L, Mallikarjun P, Joseph V, White TP, Liddle PF (2011): Regional contraction of brain surface area involves three large-scale networks in schizophrenia. *Schizophr Res*. 129: 163–168.
12. Menon V (2015): Salience Network. *Brain Mapp*. Elsevier, pp 597–611.
13. Uddin LQ (2015): Salience processing and insular cortical function and dysfunction. *Nat Rev Neurosci*. 16: 55–61.

14. Manoliu A, Riedl V, Zherdin A, Mühlau M, Schwerthöffer D, Scherr M, *et al.* (2014): Aberrant dependence of default mode/central executive network interactions on anterior insular salience network activity in schizophrenia. *Schizophr Bull*. 40: 428–437.
15. Orliac F, Naveau M, Joliot M, Delcroix N, Razafimandimby A, Brazo P, *et al.* (2013): Links among resting-state default-mode network, salience network, and symptomatology in schizophrenia. *Schizophr Res*. 148: 74–80.
16. Wotruba D, Michels L, Buechler R, Metzler S, Theodoridou A, Gerstenberg M, *et al.* (2014): Aberrant coupling within and across the default mode, task-positive, and salience network in subjects at risk for psychosis. *Schizophr Bull*. 40: 1095–1104.
17. Kapur S (2003): Psychosis as a state of aberrant salience: a framework linking biology, phenomenology, and pharmacology in schizophrenia. *Am J Psychiatry*. 160: 13–23.
18. Buckner RL, Andrews-Hanna JR, Schacter DL (2008): The Brain's Default Network. *Ann N Y Acad Sci*. 1124: 1–38.
19. Zhou Y, Liang M, Tian L, Wang K, Hao Y, Liu H, *et al.* (2007): Functional disintegration in paranoid schizophrenia using resting-state fMRI. *Schizophr Res*. 97: 194–205.
20. Garrity AG, Pearlson GD, McKiernan K, Lloyd D, Kiehl KA, Calhoun VD (2007): Aberrant "default mode" functional connectivity in schizophrenia. *Am J Psychiatry*. 164: 450–457.
21. Harrison BJ, Yücel M, Pujol J, Pantelis C (2007): Task-induced deactivation of midline cortical regions in schizophrenia assessed with fMRI. *Schizophr Res*. 91: 82–86.
22. Bressler SL, Menon V (2010): Large-scale brain networks in cognition: emerging methods and principles. *Trends Cogn Sci*. 14: 277–290.
23. Hilker R, Helenius D, Fagerlund B, Skytthe A, Christensen K, Werge TM, *et al.* (2018): Heritability of Schizophrenia and Schizophrenia Spectrum Based on the Nationwide Danish Twin Register. *Biol Psychiatry*. 83: 492–498.
24. International Schizophrenia Consortium, Purcell SM, Wray NR, Stone JL, Visscher PM, O'Donovan MC, *et al.* (2009): Common polygenic variation contributes to risk of schizophrenia and bipolar disorder. *Nature*. 460: 748–752.
25. Schizophrenia Working Group of the Psychiatric Genomics Consortium (2014): Biological insights from 108 schizophrenia-associated genetic loci. *Nature*. 511: 421–427.
26. Van der Auwera S, Wittfeld K, Shumskaya E, Bralten J, Zwiers MP, Onnink AMH, *et al.* (2017): Predicting brain structure in population-based samples with biologically informed genetic scores for schizophrenia. *Am J Med Genet Part B Neuropsychiatr Genet Off Publ Int Soc Psychiatr Genet*. 174: 324–332.
27. Van der Auwera S, Wittfeld K, Homuth G, Teumer A, Hegenscheid K, Grabe HJ (2015): No association between polygenic risk for schizophrenia and brain volume in the general population. *Biol Psychiatry*. 78: e41-42.

28. Alloza C, Cox SR, Blesa Cábez M, Redmond P, Whalley HC, Ritchie SJ, *et al.* (2018): Polygenic risk score for schizophrenia and structural brain connectivity in older age: A longitudinal connectome and tractography study. *NeuroImage*. . doi: 10.1016/j.neuroimage.2018.08.075.
29. McIntosh AM, Gow A, Luciano M, Davies G, Liewald DC, Harris SE, *et al.* (2013): Polygenic risk for schizophrenia is associated with cognitive change between childhood and old age. *Biol Psychiatry*. 73: 938–943.
30. Neilson E, Shen X, Cox SR, Clarke T-K, Wigmore EM, Gibson J, *et al.* (2019): Impact of Polygenic Risk for Schizophrenia on Cortical Structure in UK Biobank. *Biol Psychiatry*. 0. doi: 10.1016/j.biopsych.2019.04.013.
31. Ritchie SJ, Tucker-Drob EM, Cox SR, Dickie DA, Hernández M del CV, Corley J, *et al.* (2017): Risk and protective factors for structural brain ageing in the eighth decade of life. *Brain Struct Funct*. 1–14.
32. Cox SR, Bastin ME, Ferguson KJ, Allerhand M, Royle NA, Maniega SM, *et al.* (2015): Compensation or inhibitory failure? Testing hypotheses of age-related right frontal lobe involvement in verbal memory ability using structural and diffusion MRI. *Cortex J Devoted Study Nerv Syst Behav*. 63: 4–15.
33. Hoffman P, Cox SR, Dykiert D, Muñoz Maniega S, Valdés Hernández MC, Bastin ME, *et al.* (2017): Brain grey and white matter predictors of verbal ability traits in older age: The Lothian Birth Cohort 1936. *NeuroImage*. 156: 394–402.
34. Miller KL, Alfaro-Almagro F, Bangerter NK, Thomas DL, Yacoub E, Xu J, *et al.* (2016): Multimodal population brain imaging in the UK Biobank prospective epidemiological study. *Nat Neurosci*. 19: 1523–1536.
35. Kirkpatrick B, Messias E, Harvey PD, Fernandez-Egea E, Bowie CR (2008): Is Schizophrenia a Syndrome of Accelerated Aging? *Schizophr Bull*. 34: 1024–1032.
36. Kochunov P, Glahn DC, Rowland LM, Olvera RL, Winkler A, Yang Y-H, *et al.* (2013): Testing the hypothesis of accelerated cerebral white matter aging in schizophrenia and major depression. *Biol Psychiatry*. 73: 482–491.
37. Tucker-Drob EM (2013): How Many Pathways Underlie Socioeconomic Differences in the Development of Cognition and Achievement? *Learn Individ Differ*. 25: 12–20.
38. Jöreskog KG, Goldberger AS (1975): Estimation of a Model with Multiple Indicators and Multiple Causes of a Single Latent Variable. *J Am Stat Assoc*. 70: 631–639.
39. Rosseel Y (2012): lavaan: An R Package for Structural Equation Modeling. *J Stat Softw*. 48: 36.
40. Ho D, Imai K, King G, Stuart EA (2011): MatchIt: Nonparametric Preprocessing for Parametric Causal Inference. *J Stat Softw*. 42: 1–28.
41. Allen M, Poggiali D, Whitaker K, Marshall TR, Kievit R (2018): *Raincloud plots: a multi-platform tool for robust data visualization*. PeerJ Inc. doi: 10.7287/peerj.preprints.27137v1.

42. Nuevo R, Os JV, Arango C, Chatterji S, Ayuso-Mateos JL (2013, June 1): Evidence for the early clinical relevance of hallucinatory-delusional states in the general population. *Acta Psychiatr Scand*. . doi: 10.1111/acps.12010.

43. Benjamini Y, Hochberg Y (1995): Controlling the False Discovery Rate: A Practical and Powerful Approach to Multiple Testing. *J R Stat Soc Ser B Methodol*. 57: 289–300.

44. Desikan RS, Ségonne F, Fischl B, Quinn BT, Dickerson BC, Blacker D, *et al.* (2006): An automated labeling system for subdividing the human cerebral cortex on MRI scans into gyral based regions of interest. *NeuroImage*. 31: 968–980.

45. Muñoz Maniega S, Lymer GKS, Bastin ME, Marjoram D, Job DE, Moorhead TWJ, *et al.* (2008): A diffusion tensor MRI study of white matter integrity in subjects at high genetic risk of schizophrenia. *Schizophr Res*. 106: 132–139.

46. Reus LM, Shen X, Gibson J, Wigmore E, Ligthart L, Adams MJ, *et al.* (2017): Association of polygenic risk for major psychiatric illness with subcortical volumes and white matter integrity in UK Biobank. *Sci Rep*. 7. doi: 10.1038/srep42140.

47. Terwisscha van Scheltinga A, Bakker SC, van Haren NEM, Derks EM, Buizer-Voskamp JE, Boos HBM, *et al.* (2013): Genetic schizophrenia risk variants jointly modulate total brain and white matter volume. *Biol Psychiatry*. 73: 525–531.

48. Hulshoff Pol HE, Brans RGH, van Haren NEM, Schnack HG, Langen M, Baaré WFC, *et al.* (2004): Gray and white matter volume abnormalities in monozygotic and same-gender dizygotic twins discordant for schizophrenia. *Biol Psychiatry*. 55: 126–130.

49. McGrath JJ, Saha S, Al-Hamzawi A, Alonso J, Bromet EJ, Bruffaerts R, *et al.* (2015): Psychotic Experiences in the General Population: A Cross-National Analysis Based on 31,261 Respondents From 18 Countries. *JAMA Psychiatry*. 72: 697–705.

50. Nuevo R, Chatterji S, Verdes E, Naidoo N, Arango C, Ayuso-Mateos JL (2012): The continuum of psychotic symptoms in the general population: a cross-national study. *Schizophr Bull*. 38: 475–485.

51. Critchley HD, Wiens S, Rotshtein P, Ohman A, Dolan RJ (2004): Neural systems supporting interoceptive awareness. *Nat Neurosci*. 7: 189–195.

52. Damasio A (2003): Mental self: The person within. *Nature*. 423: 227.

53. Costafreda SG, Brébion G, Allen P, McGuire PK, Fu CHY (2008): Affective modulation of external misattribution bias in source monitoring in schizophrenia. *Psychol Med*. 38: 821–824.

54. Johns LC, Rossell S, Frith C, Ahmad F, Hemsley D, Kuipers E, McGuire PK (2001): Verbal self-monitoring and auditory verbal hallucinations in patients with schizophrenia. *Psychol Med*. 31: 705–715.

55. Crespo-Facorro B, Kim J, Andreasen NC, O'Leary DS, Bockholt HJ, Magnotta V (2000): Insular cortex abnormalities in schizophrenia: a structural magnetic resonance imaging study of first-episode patients. *Schizophr Res*. 46: 35–43.

56. Díaz-Caneja CM, Schnack H, Martínez K, Santonja J, Alemán-Gomez Y, Pina-Camacho L, *et al.* (2019): Neuroanatomical deficits shared by youth with autism spectrum disorders and psychotic disorders. *Hum Brain Mapp*. 40: 1643–1653.

57. Crespo-Facorro B, Roiz-Santiáñez R, Quintero C, Pérez-Iglesias R, Tordesillas-Gutiérrez D, Mata I, *et al.* (2010): Insular cortex morphometry in first-episode schizophrenia-spectrum patients: Diagnostic specificity and clinical correlations. *J Psychiatr Res*. 44: 314–320.

58. Sommer IEC, Diederen KMJ, Blom J-D, Willems A, Kushan L, Slotema K, *et al.* (2008): Auditory verbal hallucinations predominantly activate the right inferior frontal area. *Brain*. 131: 3169–3177.

59. Paulesu E, Frith CD, Frackowiak RS (1993): The neural correlates of the verbal component of working memory. *Nature*. 362: 342–345.

60. Gaser C, Nenadic I, Volz H-P, Büchel C, Sauer H (2004): Neuroanatomy of "hearing voices": a frontotemporal brain structural abnormality associated with auditory hallucinations in schizophrenia. *Cereb Cortex N Y N 1991*. 14: 91–96.

61. Diederen KMJ, Neggers SFW, de Weijer AD, van Lutterveld R, Daalman K, Eickhoff SB, *et al.* (2013): Aberrant resting-state connectivity in non-psychotic individuals with auditory hallucinations. *Psychol Med*. 43: 1685–1696.

62. van Lutterveld R, Diederen KMJ, Otte WM, Sommer IE (2014): Network analysis of auditory hallucinations in nonpsychotic individuals. *Hum Brain Mapp*. 35: 1436–1445.

63. Francis AN, Seidman LJ, Jabbar GA, Mesholam-Gately R, Thermenos HW, Juelich R, *et al.* (2012): Alterations in brain structures underlying language function in young adults at high familial risk for schizophrenia. *Schizophr Res*. 141: 65–71.

64. Padmanabhan JL, Tandon N, Haller CS, Mathew IT, Eack SM, Clementz BA, *et al.* (2015): Correlations Between Brain Structure and Symptom Dimensions of Psychosis in Schizophrenia, Schizoaffective, and Psychotic Bipolar I Disorders. *Schizophr Bull*. 41: 154–162.

65. Hoffman RE, Rapaport J, Mazure CM, Quinlan DM (1999): Selective speech perception alterations in schizophrenic patients reporting hallucinated "voices." *Am J Psychiatry*. 156: 393–399.

66. Zmigrod L, Garrison JR, Carr J, Simons JS (2016): The neural mechanisms of hallucinations: A quantitative meta-analysis of neuroimaging studies. *Neurosci Biobehav Rev*. 69: 113–123.

67. Corlett PR, Horga G, Fletcher PC, Alderson-Day B, Schmack K, Powers AR (2019): Hallucinations and Strong Priors. *Trends Cogn Sci*. 23: 114–127.

68. Bohland JW, Bokil H, Allen CB, Mitra PP (2009): The brain atlas concordance problem: quantitative comparison of anatomical parcellations. *PloS One*. 4: e7200.

69. Cox SR, Ferguson KJ, Royle NA, Shenkin SD, MacPherson SE, MacLullich AMJ, *et al.* (2014): A systematic review of brain frontal lobe parcellation techniques in magnetic resonance imaging. *Brain Struct Funct*. 219: 1–22.

70. de Reus MA, van den Heuvel MP (2013): The parcellation-based connectome: limitations and extensions. *NeuroImage*. 80: 397–404.
71. Goulas A, Uylings HBM, Hilgetag CC (2017): Principles of ipsilateral and contralateral cortico-cortical connectivity in the mouse. *Brain Struct Funct*. 222: 1281–1295.
72. Buchanan CR, Bastin ME, Ritchie SJ, Liewald DC, Madole J, Tucker-Drob EM, *et al.* (2019): The effect of network thresholding and weighting on structural brain networks in the UK Biobank. *bioRxiv*. . doi: 10.1101/649418.
73. Fry A, Littlejohns TJ, Sudlow C, Doherty N, Adamska L, Sprosen T, *et al.* (2017): Comparison of Sociodemographic and Health-Related Characteristics of UK Biobank Participants With Those of the General Population. *Am J Epidemiol*. 186: 1026–1034.
74. Menon V, Uddin LQ (2010): Saliency, switching, attention and control: a network model of insula function. *Brain Struct Funct*. 214: 655–667.
75. Catani M, Dell'acqua F, Thiebaut de Schotten M (2013): A revised limbic system model for memory, emotion and behaviour. *Neurosci Biobehav Rev*. 37: 1724–1737.
76. Power JD, Cohen AL, Nelson SM, Wig GS, Barnes KA, Church JA, *et al.* (2011): Functional network organization of the human brain. *Neuron*. 72: 665–678.
77. Sridharan D, Levitin DJ, Menon V (2008): A critical role for the right fronto-insular cortex in switching between central-executive and default-mode networks. *Proc Natl Acad Sci U S A*. 105: 12569–12574.

Tables

Table 1 Selected networks and their corresponding nodes.

Network	Nodes implicated	References
Salience	Thalamus, amygdala, VentralDC, caudal anterior cingulate and insula	Menon, 2015; Menon and Uddin, 2010
Default mode	Lateral orbitofrontal, medial orbito frontal, middle temporal, pars orbitalis, posterior cingulate and supramarginal	Bressler and Menon, 2010; Catani et al., 2013
Central-Executive	Caudal middle frontal, inferior parietal, rostral middle frontal, superior frontal and superior parietal	Menon and Uddin, 2010; Power et al., 2011; Sridharan et al., 2008

Note: VentralDC = Ventral diencephalon

Table 2. Participants characteristics

	Variable	Units	Descriptor	Valid N
Demographics	Age	Years (SD)	62.18 (7.57)	3875
	Sex	F, % Females	2032 (52.44)	3875
PLEs	Conspiratorial thoughts	Yes (% Yes)	16 (0.41%) [a]	13:130 [b]
	Unusual signs	Yes (% Yes)	13 (0.34%) [a]	11:110 [b]
	Unusual voices	Yes (% Yes)	55 (1.42%) [a]	51:510 [b]
	Unusual visions	Yes (% Yes)	79 (2.04%) [a]	70:700 [b]
Brain MRI	Cortical thickness	mm Mean (SD)	2.40 (0.10)	3566
	Grey matter volume	mm^3 Mean (SD)	620504.60 (55712.52)	3868
	Mean FA	Units (SD)	0.46 (0.02)	3174

Note: SD = standard deviation. Brain MRI volumes are uncorrected for head size. [a] Percentages and rates were calculated based on the total sample of N = 3869. [b] Due to the relatively low frequencies of PLEs in this sample, participants were matched 1:10.

Figures

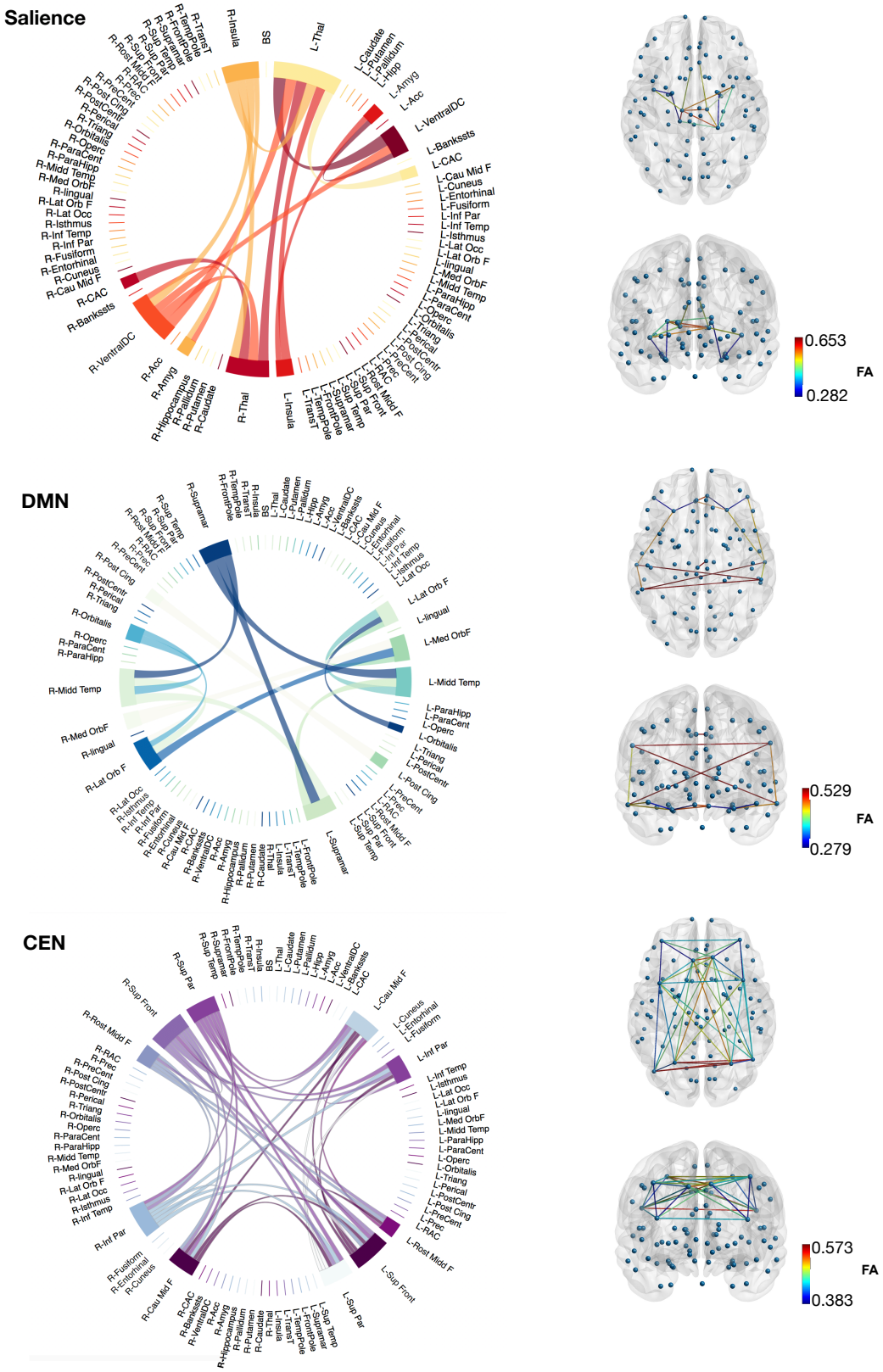
Salience
R-Insula
BS
L-Thal
L-Caudate
L-Putamen
L-Pallidum
L-Hipp
L-Amyg
L-Acc
L-VentralDC
L-Bankssts
L-CAC
L-Cau Mid F
L-Cuneus
L-Entorhinal
L-Fusiform
L-Inf Par
L-Inf Temp
L-Isthmus
L-Lat Occ
L-Lat Orb F
L-lingual
L-Med OrbF
L-Midd Temp
L-ParaHipp
L-ParaCent
L-Operc
L-Orbitalis
L-Triang
L-Perical
L-PostCentr
L-Post Cing
L-PreCent
L-Prec
L-RAC
L-Rost Midd F
L-Sup Front
L-Sup Par
L-Sup Temp
L-Supramar
L-FromPole
L-TemPole
L-TransT
L-Insula
L-Thal
R-Thal
R-Caudate
R-Putamen
R-Pallidum
R-Hippocampus
R-Amyg
R-Acc
R-VentralDC
R-Bankssts
R-CAC
R-Cau Mid F
R-Cuneus
R-Entorhinal
R-Fusiform
R-Inf Par
R-Inf Temp
R-Isthmus
R-Lat Occ
R-Lat Orb F
R-lingual
R-Med OrbF
R-Midd Temp
R-ParaHipp
R-ParaCent
R-Operc
R-Orbitalis
R-Triang
R-Perical
R-PostCentr
R-Post Cing
R-PreCent
R-Prec
R-RAC
R-Rost Midd F
R-Sup Front
R-Sup Par
R-Sup Temp
R-Supramar
R-FromPole
R-TemPole
R-TransT
0.653
FA
0.282
DMN
R-Supramar
R-Sup Temp
R-Sup Par
R-Sup Front
R-Rost Midd F
R-RAC
R-Prec
R-PreCent
R-Post Cing
R-PostCentr
R-Perical
R-Triang
R-Orbitalis
R-Operc
R-ParaCent
R-ParaHipp
R-Midd Temp
R-Med OrbF
R-lingual
R-Lat Orb F
R-Lat Occ
R-Isthmus
R-Inf Temp
R-Inf Par
R-Fusiform
R-Entorhinal
R-Cuneus
R-Cau Mid F
R-CAC
R-Bankssts
R-VentralDC
R-Acc
R-Amyg
R-Hippocampus
R-Pallidum
R-Putamen
R-Caudate
R-Thal
R-Insula
R-TransT
R-TemPole
R-FromPole
BS
L-Thal
L-Caudate
L-Putamen
L-Pallidum
L-Hipp
L-Amyg
L-Acc
L-VentralDC
L-Bankssts
L-CAC
L-Cau Mid F
L-Cuneus
L-Entorhinal
L-Fusiform
L-Inf Par
L-Inf Temp
L-Isthmus
L-Lat Occ
L-Lat Orb F
L-lingual
L-Med OrbF
L-Midd Temp
L-ParaHipp
L-ParaCent
L-Operc
L-Orbitalis
L-Triang
L-Perical
L-PostCentr
L-Post Cing
L-PreCent
L-Prec
L-RAC
L-Rost Midd F
L-Sup Front
L-Sup Par
L-Sup Temp
L-Supramar
L-FromPole
L-TemPole
L-TransT
L-Insula
0.529
FA
0.279
CEN
R-Sup Temp
R-Supramar
R-FromPole
R-TemPole
R-TransT
R-Insula
BS
L-Thal
L-Caudate
L-Putamen
L-Pallidum
L-Hipp
L-Amyg
L-Acc
L-VentralDC
L-Bankssts
L-CAC
L-Cau Mid F
L-Cuneus
L-Entorhinal
L-Fusiform
L-Inf Par
L-Inf Temp
L-Isthmus
L-Lat Occ
L-Lat Orb F
L-lingual
L-Med OrbF
L-Midd Temp
L-ParaHipp
L-ParaCent
L-Operc
L-Orbitalis
L-Triang
L-Perical
L-PostCentr
L-Post Cing
L-PreCent
L-Prec
L-RAC
L-Rost Midd F
L-Sup Front
L-Sup Par
L-Sup Temp
L-Supramar
L-FromPole
L-TemPole
L-TransT
L-Insula
R-Thal
R-Caudate
R-Putamen
R-Pallidum
R-Hippocampus
R-Amyg
R-Acc
R-VentralDC
R-Bankssts
R-CAC
R-Cau Mid F
R-Cuneus
R-Entorhinal
R-Fusiform
R-Inf Par
R-Inf Temp
R-Isthmus
R-Lat Occ
R-Lat Orb F
R-lingual
R-Med OrbF
R-Midd Temp
R-ParaHipp
R-ParaCent
R-Operc
R-Orbitalis
R-Triang
R-Perical
R-PostCentr
R-Post Cing
R-PreCent
R-Prec
R-RAC
R-Rost Midd F
R-Sup Front
R-Sup Par
0.573
FA
0.383

Figure 1 Diagram of nodes of interest and their linking pathways derived from the connectome for the networks of interest. Colours were randomly assigned, and width of the links are proportional to mean FA values across all participants. Axial and coronal views of the networks with colour-coded FA gradient. L: left, R: right. A list of abbreviations is provided in Supplementary Material Table 2.

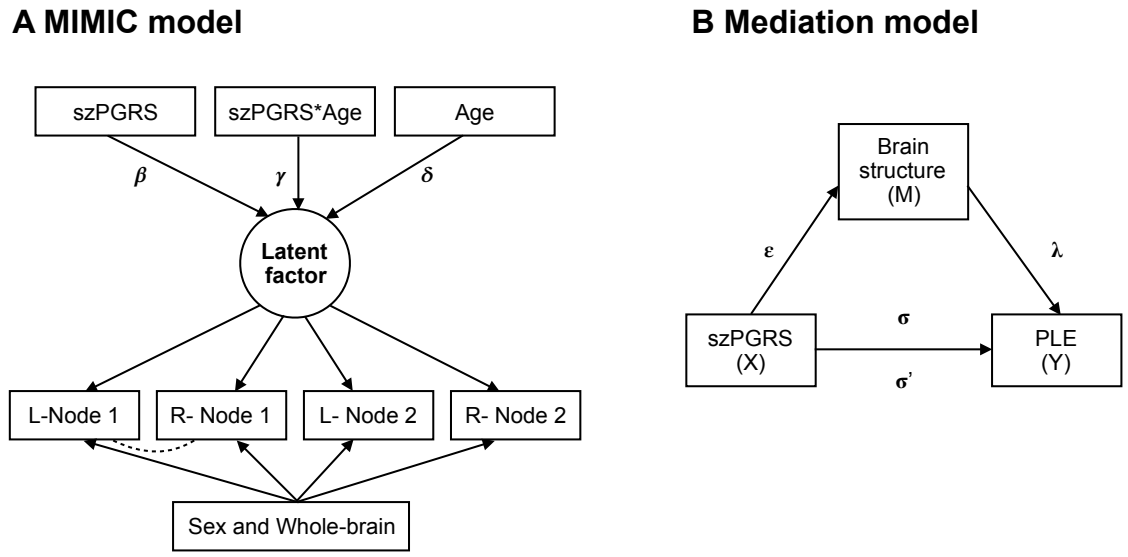

Figure 2 Diagrams of structural equation models (SEM). A. Multiple indicators, multiple causes (MIMIC) model (38) for neurostructural properties of each network. A separate model was applied to FA, grey matter thickness and grey matter volume. From each individual bilateral node (L: left; R: right) or pathway, a latent score was calculated for FA, grey matter thickness and grey matter volume controlling for sex and whole-brain structural properties at the manifest level (i.e: whole brain cortical thickness/volume/FA). Relation between FA/thickness/volume and szPGRS is indicated by path β; path γ represents the association between the interaction of age and szPGRS and FA/thickness/volume factors; path δ represents the association between age and the latent factor. szPGRS was corrected for sex and population stratification (paths not shown). The dashed line represents a possible residual correlation between nodes. **B.** Path diagram of mediation model, where the ε coefficient represents the

regression of X on M, λ coefficient the regression of M on Y and σ coefficient the direct path of X on Y. The product of the ε and λ coefficients describes the indirect path of X on Y through M (σ').

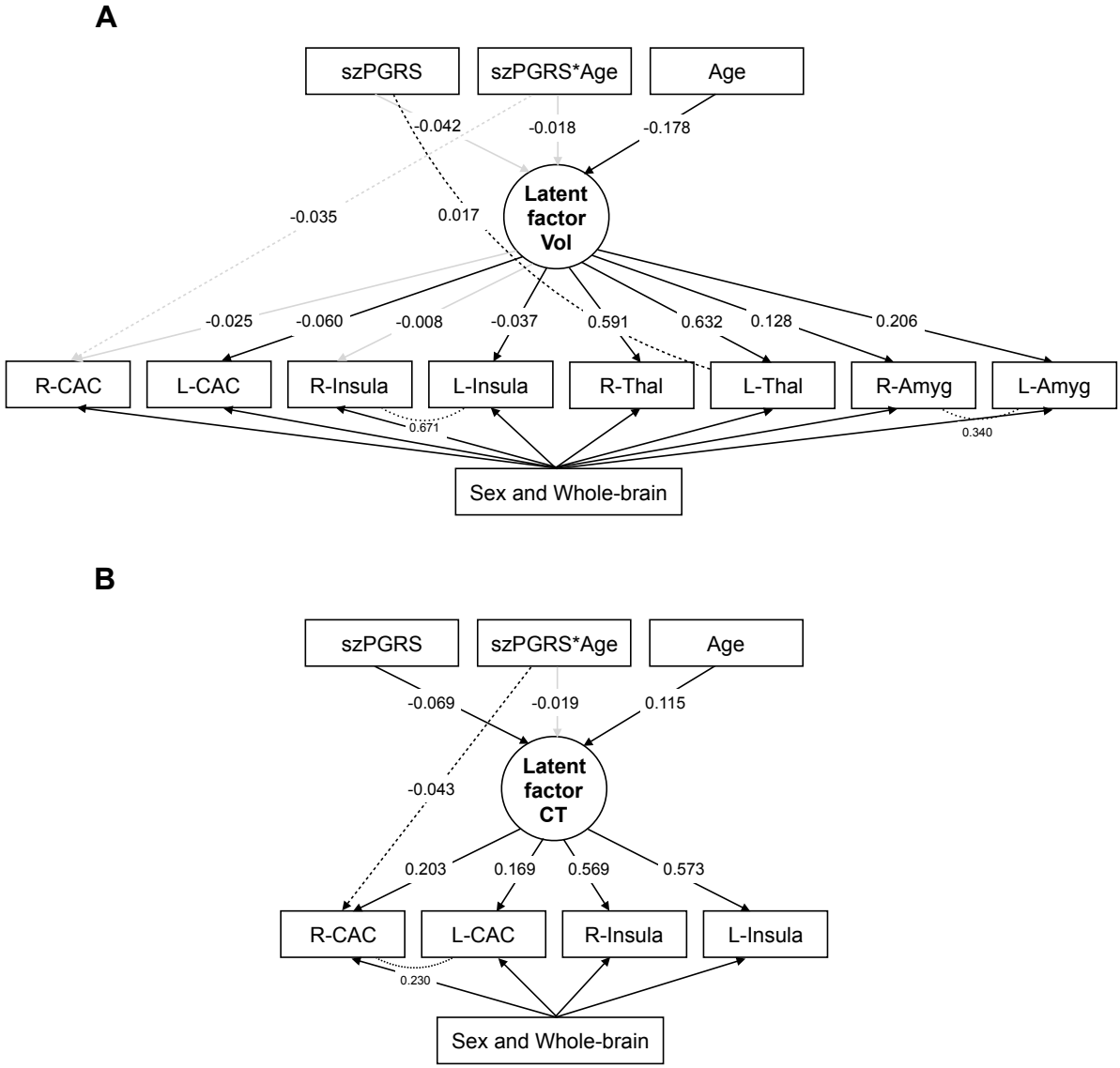

Figure 3 Diagrams of MIMIC and independent pathway models of the salience network. **A.** Common + independent pathways model for latent factor of grey matter thickness. **B.** Common + independent pathways model for latent factor of grey matter volume. Dashed lines represent

independent pathways while dotted lines residual correlations between nodes. Black lines represent statistically significant pathways ($p < 0.050$) while grey lines non-significant pathways ($p > 0.050$).

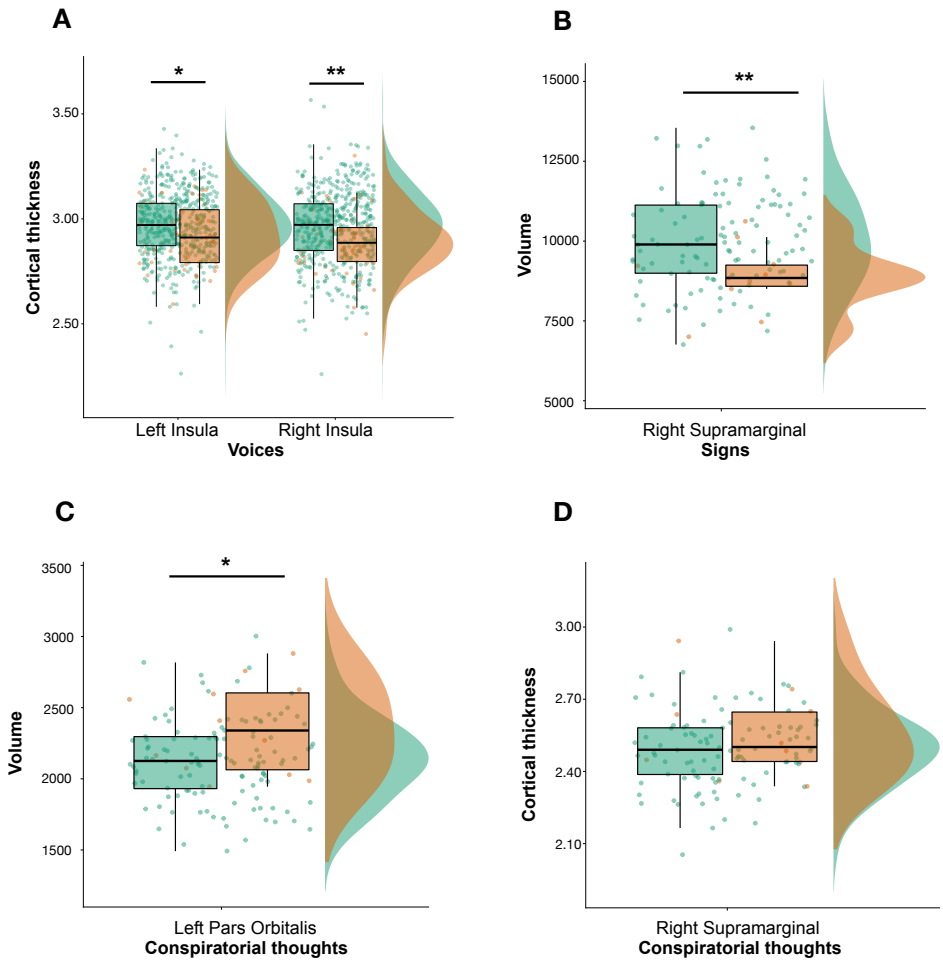

Figure 4: Raincloud plots representing differences in cortical thickness and volume between participants reporting PLEs (orange) and matched controls (green). **A** Bilateral cortical thickness of the insula and voices. **B** Volume of right supramarginal gyrus and unusual signs. **C** Volume of the left pars orbitalis and conspiratorial thoughts. **D** Cortical thickness of the right supramarginal gyrus and conspiratorial thoughts. *Note*: CAC: caudal anterior cingulate. Cortical thickness is measured in cm and volume in cm^3. Asterisks represent significant differences between groups (*: $p < 0.05$, **: $p < 0.01$).

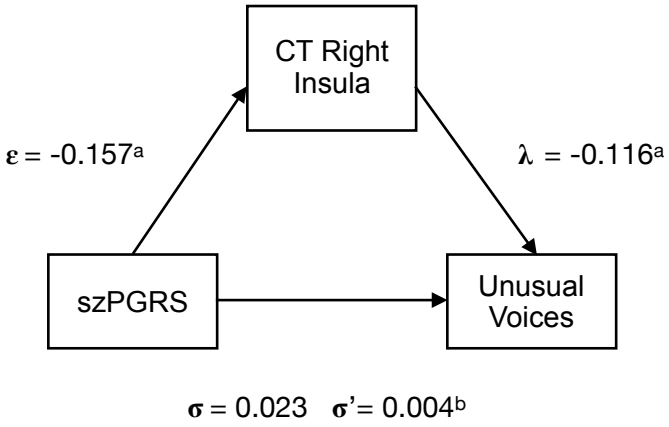

Figure 5: Path diagram of the mediation model, where the ε coefficient represents the coefficient of regressions of szPGRS on cortical thickness of the right insula, and λ the coefficient of the regression of cortical thickness of the right insula on unusual voices and σ coefficient of the direct path of szPGRS and unusual voices. Coefficient of σ' represents the indirect path of szPGRS on unusual signs through cortical thickness of the right insula. *Note:* CT = cortical thickness, [a] *p* values < 0.05, [b] Confidence intervals not including zero.